Analyst

PAPER

Facile magnetization of metal–organic framework MIL-101 for magnetic solid-phase extraction of polycyclic aromatic hydrocarbons in environmental water samples

Shu-Hui Huo and Xiu-Ping Yan*

The unusual properties such as high surface area, good thermal stability, uniform structured nanoscale cavities and the availability of in-pore functionality and outer-surface modification make metal–organic frameworks (MOFs) attractive for diverse analytical applications. However, integration of MOFs with magnets for magnetic solid-phase extraction for analytical application has not been attempted so far. Here we show a facile magnetization of MOF MIL-101(Cr) for rapid magnetic solid-phase extraction of polycyclic aromatic hydrocarbons (PAHs) from environmental water samples. MIL-101 is attractive as a sorbent for solid-phase extraction of pollutants in aqueous solution due to its high surface area, large pores, accessible coordinative unsaturated sites, and excellent chemical and solvent stability. *In situ* magnetization of MIL-101 microcrystals as well as magnetic solid-phase extraction of PAHs was achieved simultaneously by simply mixing MIL-101 and silica-coated Fe_3O_4 microparticles in a sample solution under sonication. Such MOF-based magnetic solid-phase extraction in combination with high-performance liquid chromatography gave the detection limits of 2.8–27.2 ng L^{-1} and quantitation limits of 6.3–87.7 ng L^{-1} for the PAHs. The relative standard deviations for intra- and inter-day analyses were in the range of 3.1–8.7% and 6.1–8.5%, respectively. The results showed that hydrophobic and π–π interactions between the PAHs and the framework terephthalic acid molecules, and the π-complexation between PAHs and the Lewis acid sites in the pores of MIL-101 play a significant role in the adsorption of PAHs.

Introduction

Metal–organic frameworks (MOFs) are an intriguing class of hybrid material that exist as infinite crystalline lattices with metal clusters and organic linkers, and possess accessible cages, tunnels and modifiable pores.[1–4] Their unique characteristics make MOFs promising for diverse applications in analytical chemistry.[5] MOFs have been successfully explored as sorbents for sampling,[6,7] solid-phase extraction (SPE),[8,9] solid-phase microextraction,[10–12] and as stationary phases for gas chromatography[11,13–17] and liquid chromatography.[18–22]

Magnetic separation based on magnetic nanoparticles has received considerable attention mainly due to its speed, compatibility and especially for its high selectivity when used on complex matrices.[23–25] In many cases, magnetic nanoparticles functionalized with different groups are used for the preconcentration and isolation of analytes.[25,26] As magnetic separation is directly performed on complex samples, the high back pressure created by passing a water sample through the columns

State Key Laboratory of Medicinal Chemical Biology, Research Center for Analytical Sciences, College of Chemistry, Nankai University, Tianjin 300071, China. E-mail: xpyan@nankai.edu.cn; Fax: +86 22-23506075; Tel: +86 22-23506075

packed with nanosized adsorbents in conventional SPE is avoided.[25] Owing to the merits of magnetic separation, the combination of magnetic nanoparticles with SPE, magnetic SPE (MSPE), has attracted much attention due to its great potential applications in preconcentration and separation.[26–39] Magnetic retrieval of some sorbents such as graphene, oxidized carbon nanotubes and chitosan has been reported.[28–30] Considering the unique properties of MOFs, subtle coupling of MOFs and MSPE will be interesting and significant for SPE applications. However, the use of intrinsic magnetic properties of MOFs for magnetic separation seems infeasible due to their limited magnetization. The magnetic functionalization of MOFs is thus necessary for magnetic separation. Lohe *et al.*[23] achieved magnetic functionalization of MOFs through the heteronucleation of the porous networks on the outer surface of the magnetic nanoparticles for catalyst separation and drug release. However, to the best of our knowledge, the utilization of MOFs as sorbents for MSPE has not been reported for analytical application so far.

Here we report a facile magnetization of MOF MIL-101 for rapid MSPE of polycyclic aromatic hydrocarbons (PAHs) in environmental water samples. PAHs were selected as the analytes because of their toxic, mutagenic and carcinogenic effects.[40] The determination of PAHs in environmental aqueous solutions is

a major challenge because of their low solubility and low concentration levels in water.[41] Therefore, effective preconcentration and separation of PAHs by SPE with various sorbents have received great attention.[8,12,26,37–39,42–52] MIL-101 was used as an example of MOFs due to its attractive features as a sorbent for the extraction of pollutants in aqueous solution, such as high surface area, large pore windows (12 Å and 16 Å × 14.5 Å), large pores (29 Å and 34 Å), accessible coordinative unsaturated sites, and excellent chemical and solvent stability.[20,53] In this work, we simultaneously achieved *in situ* magnetization of MIL-101 microcrystals as well as MSPE of PAHs by simply mixing MIL-101 and silica-coated Fe_3O_4 microparticles in aqueous sample solution under sonication. The preparation, characterization of MIL-101, silica-coated magnetic microparticles ($Fe_3O_4@SiO_2$) and magnetically functionalized MIL-101 ($Fe_3O_4@SiO_2$–MIL-101) were studied. The potential factors affecting the performance of the $Fe_3O_4@SiO_2$–MIL-101 on the MSPE of PAHs in environmental water samples were evaluated in detail.

Experimental

Chemicals and materials

All chemicals were at least of analytical grade. $Cr(NO_3)_3\cdot9H_2O$, terephthalic acid, and hydrofluoric acid (Aladdin, Shanghai, China) were used to prepare MIL-101. Ferric chloride hexahydrate ($FeCl_3\cdot6H_2O$), glycol, polyethylene glycol, and anhydrous sodium acetate (Guangfu, Tianjin, China) were used to prepare magnetic Fe_3O_4 microparticles. Tetraethylorthosilicate (TEOS) was used for further modification of the magnetic Fe_3O_4 microparticles. Methanol, acetonitrile, acetone, and anhydrous ethanol were obtained from Concord Technology (Tianjin, China). Ultrapure water (18.2 MΩ cm) was obtained from a WaterPro Water Purification System (Labconco Corporation, Kansas City, MO, USA). Naphthalene (Nap), acenaphthene (Ace), anthracene (Ant), fluoranthene (FluA), and pyrene (Pyr), benz[*a*]anthracene (BaA) were purchased from Tianchang Chemical Co., Ltd. (Anshan, Liaoning, China). Individual stock solutions of the PAHs were prepared by dissolving 5.0 mg of the pure analytical standards in 10 mL of acetonitrile. The working standard solution was prepared by combining aliquots of each individual stock solutions and diluting to obtain a desired concentration. The volume portion of acetonitrile in any working solution was kept less than 1%. The solutions mentioned above were kept at 4 °C in the dark. **Caution**: take care to avoid direct contact with all the analytes studied and prepare all the solutions in a well-ventilated hood because of their high toxicity.

Apparatus

The chromatographic system consisted of a Waters 600 HPLC pump and a Waters 2996 photodiode array (PDA) detector (Milford, MA, USA). All separations were achieved on an analytical reversed-phase C18 column (5 μm particle diameter, 4.6 mm i.d. × 15 cm long) supplied by Baseline Technologies (Tianjin, China) at a flow rate of 1.0 mL min⁻¹ mobile phase under isocratic conditions at room temperature. The Empower software was used to acquire and process spectral and chromatographic data. The photodiode array detector was operated between 210 and 400 nm. Multiple wavelengths were used for the

quantification of PAHs: 220 nm for naphthalene, 227.5 nm for acenaphthene, 252 nm for anthracene, 240 nm for fluoranthene and pyrene, and 287 nm for benzanthracene. Best chromatographic resolution for the separation of PAHs was obtained with a mixture of methanol and water (85 : 15) as the mobile phase. The mobile phase was filtered through a 0.45 μm nylon membrane filter prior to use. The injection volume of the sample solution was 20 μL.

The X-ray diffraction (XRD) patterns were recorded with a D/max-2500 diffractometer (Rigaku, Japan) using Cu K_α radiation ($\lambda = 1.5418$ Å) over the angular range from 3° to 80°. Transmission electron microscopic (TEM) characterization was performed on a Tecnai G2 F20 (Philips, Holland) at 200 kV. The magnetic properties were studied using a LDJ 9600-1 vibrating sample magnetometer (LDJ Electronics Inc., Troy, MI, USA) at room temperature by cycling the field from −10 to 10 kOe. Zeta potentials of the adsorbent in ultrapure water were measured on a zeta potential analyzer (Brookhaven Instruments Co., Holtsville, NY, USA). The ultrasonic device used was a KQ2200E instrument with a frequency of 40 kHz and a nominal power of 80 W (Kunshan, China). A strong Nd–Fe–B magnet (50 mm × 50 mm × 25 mm, Tianhe Magnet, Tianjin, China) was used for magnetic isolation.

Preparation of magnetic $Fe_3O_4@SiO_2$

Magnetic Fe_3O_4 microparticles (MMPs) were prepared by a solvothermal reduction method according to Li *et al.*[54] Briefly, a mixture of $FeCl_3\cdot6H_2O$ (1.35 g), anhydrous sodium acetate (3.6 g), and polyethylene glycol (1.0 g) in glycol (40 mL) was stirred vigorously for 30 min, then transferred into a Teflon-lined autoclave and reacted at 200 °C for 72 h to give Fe_3O_4 magnetic microspheres, and allowed to cool to room temperature. The black magnetic microspheres were collected, and washed with ethanol and ultrapure water four times, and then the product was dried under vacuum at 60 °C for 12 h.

The silica-coated magnetic Fe_3O_4 microspheres were prepared according to the Stöber method with some modification.[55,56] Freshly prepared magnetic Fe_3O_4 microspheres (1.0 g) were first treated with HCl aqueous solution (200 mL, 0.1 M) under ultrasonication, then washed thoroughly with ultrapure water. The magnetic microspheres were re-dispersed in a mixture of ethanol (320 mL), ultrapure water (80 mL) and $NH_3\cdot H_2O$ solution (5.0 mL, 25–28 w/w%). Then, TEOS (1 mL) was introduced to the above dispersion after ultrasonic vibration for 10 min. The reaction was allowed to proceed under mechanical stirring for 12 h. The harvested particles were collected with a magnet, washed with ethanol and ultrapure water four times.

Synthesis of MIL-101

MIL-101 was synthesized according to Férey *et al.* with a slight modification.[53] Typically, $Cr(NO_3)_3\cdot9H_2O$ (800 mg), terephthalic acid (332 mg) and hydrofluoric acid (0.1 mL, 40 w/w%) were mixed with ultrapure water (9.5 mL). The obtained mixture was transferred to a Teflon-lined bomb. Then, the Teflon-lined bomb was sealed, placed in an oven, and left at 220 °C for 8 h. The as-synthesized MIL-101 was further purified by washing with DMF and hot ethanol, and collected *via* centrifugation at
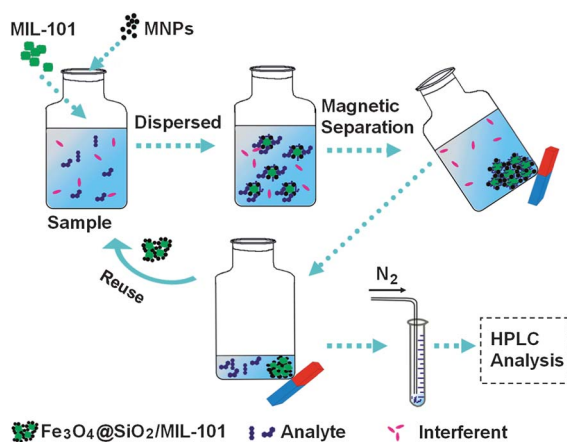
10 000 rpm for 5 min. The procedure was repeated three times to remove the unreacted terephthalic acid from MIL-101. The solid was obtained with centrifugation at 10 000 rpm for 5 min, and evacuated in vacuum at 150 °C for 12 h.

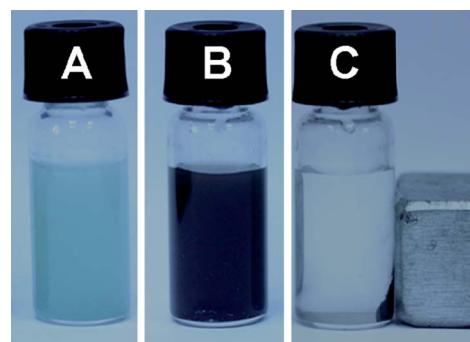### Procedure for *in situ* magnetization of MIL-101 and MSPE

Fe_3O_4@SiO_2 (1.0 mg) and MIL-101 (0.6 mg) were placed in a 25 mL glass vial, and washed with methanol and ultrapure water sequentially. To carry out the extraction, 20 mL of aqueous standard solution or sample solution was added into the vial. The vial was closed with a cap after adding sample solution. The Fe_3O_4@SiO_2 and MIL-101 were dispersed in the mixture solution under ultrasonication for 20 min for the magnetization of MIL-101 to form Fe_3O_4@SiO_2–MIL-101 microspheres for simultaneous SPE of PAHs. Then, an external magnet was attached to the outside bottom of the vial, so that the Fe_3O_4@SiO_2–MIL-101 microspheres were gathered to the bottom of the vial, and the supernatant was discarded. The analytes were desorbed from the Fe_3O_4@SiO_2–MIL-101 microspheres with 0.5 mL of acetonitrile under ultrasonication for 20 s, and the eluate was collected with magnetic separation. Three such replicate elutions were needed for quantitative desorption of the analytes from the sorbent. The collected eluate was concentrated to less than 0.1 mL with a gentle stream of nitrogen at 30 °C, diluted to 0.1 mL with the mobile phase, and filtered through a 0.45 μm nylon membrane for HPLC analysis (Scheme 1). The photographs of dispersed MIL-101 and Fe_3O_4@SiO_2–MIL-101 are shown in Fig. 1A and B, respectively. A clear supernatant was obtained after rapid separation of Fe_3O_4@SiO_2–MIL-101 with the external magnet (Fig. 1C).

Sample preparation

Lake water and wastewater samples were collected locally. All of the water samples were filtered through a 0.45 μm Millipore cellulose membrane immediately after sampling, stored in clean glass bottles, and analyzed immediately by HPLC.

Fig. 1 Photographs for dispersion of MIL-101 (A), Fe_3O_4@SiO_2–MIL-101 (B) and separation of Fe_3O_4@SiO_2–MIL-101 with magnet (C).

Results and discussion

Characterization of the prepared MIL-101, Fe_3O_4@SiO_2, and Fe_3O_4@SiO_2–MIL-101

The prepared MIL-101 was characterized by XRD (Fig. 2A), and N_2 adsorption–desorption experiment (Fig. 2B). The experimental XRD pattern of the synthesized MIL-101 is in good agreement with the simulated one, showing the successful preparation of MIL-101. The prepared MIL-101 gave a BET surface area of 2832 m^2 g^{-1} with a pore volume of 0.82 cm^3 g^{-1}. The magnetization curves of Fe_3O_4, Fe_3O_4@SiO_2, and Fe_3O_4@SiO_2–MIL-101 are shown in Fig. 2C. The saturation magnetization values for Fe_3O_4, Fe_3O_4@SiO_2, and Fe_3O_4@SiO_2–MIL-101 were 76, 38, and 21 emu g^{-1}, respectively. The relatively high saturation magnetization value of Fe_3O_4@SiO_2–MIL-101 made this kind sorbent susceptible to magnetic fields and easy to isolate from aqueous solution. The hysteresis loops without apparent hysteresis, remanence and coercivity illustrate the superparamagnetic characteristic of Fe_3O_4@SiO_2–MIL-101 MNPs, which is necessary for the magnetic extraction.

The TEM images of Fe_3O_4 MNPs, MIL-101 and Fe_3O_4@SiO_2–MIL-101 are shown in Fig. 3. The bare Fe_3O_4 MMPs were

Scheme 1 Schematic diagram for the application of Fe_3O_4@SiO_2–MIL-101 MNPs as sorbent for MSPE.
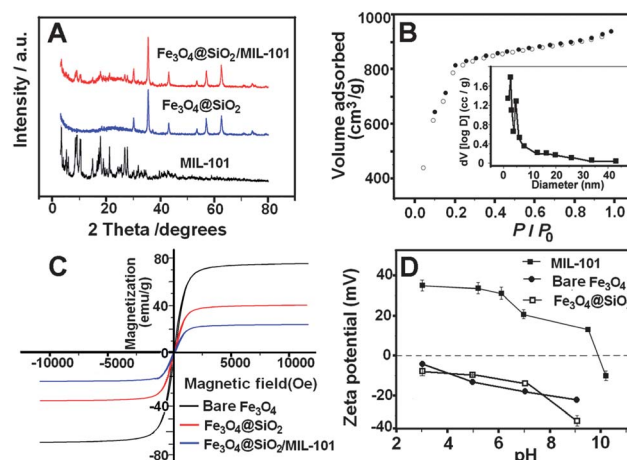
Fig. 2 (A) XRD pattern of the as-synthesized MIL-101, Fe_3O_4@SiO_2 and Fe_3O_4@SiO_2–MIL-101; (B) N_2 adsorption–desorption isotherms and the pore size distribution of the as-synthesized MIL-101 (inset); (C) magnetization curves and (D) zeta potential of Fe_3O_4, Fe_3O_4@SiO_2 and MIL-101.
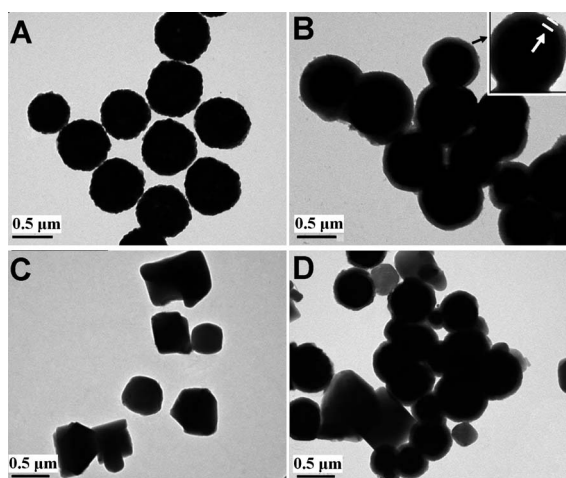
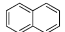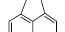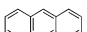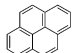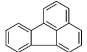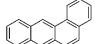**Fig. 3** TEM images of the MMPs: (A) Fe_3O_4; (B) $Fe_3O_4@SiO_2$; (C) MIL-101; and (D) $Fe_3O_4@SiO_2$–MIL-101.
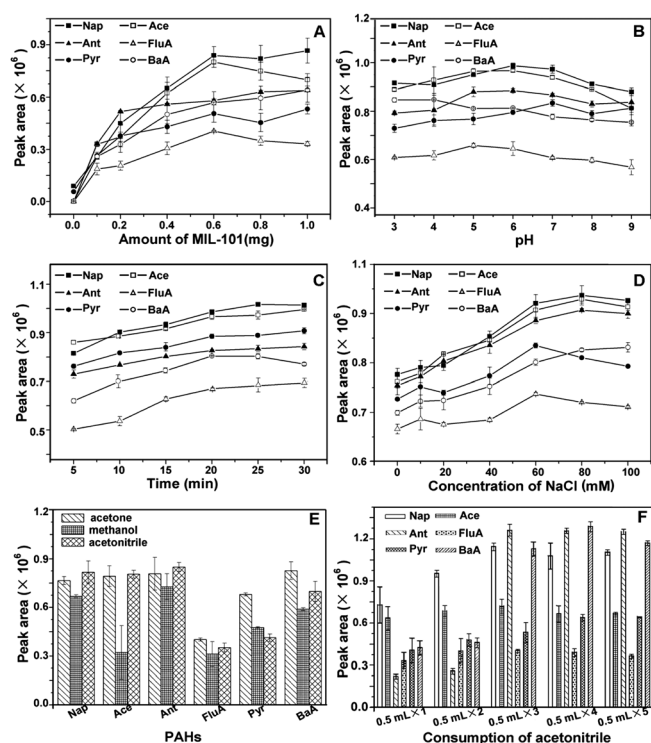
Fig. 4 Factors affecting the extraction efficiency for 50 ng mL^{-1} PAHs. (A) Effect of the amount of MIL-101. Other conditions: pH, 6.0; extraction time, 20 min; NaCl, 50 mM; desorption solvent, 1 mL acetonitrile. (B) Effect of pH. Other conditions: MIL-101, 0.6 mg; extraction time, 20 min; desorption solvent, 1 mL acetonitrile; NaCl, 50 mM. (C) Effect of extraction time. Other conditions: MIL-101, 0.6 mg; pH, 6.0; NaCl, 50 mM; desorption solvent, 1 mL acetonitrile. (D) Effect of ionic strength. Other conditions: MIL-101, 0.6 mg; pH, 6.0; extraction time, 25 min; desorption solvent, 1 mL acetonitrile. (E) Effect of eluent. (F) Effect of acetonitrile volume. Other conditions: MIL-101, 0.6 mg; pH, 6.0; extraction time, 25 min; NaCl, 60 mM. Error bars show the standard deviations for three replicate extractions.

narrowly distributed with an average size of 600 nm (Fig. 3A). A silica layer coated on the outside surface of the spherical Fe_3O_4 MMPs was observed (about 30 nm, Fig. 3B), which can be

Table 1 Physical–chemical properties of the PAHs

Analyte	Structure	Molecular weight	log K_{ow}[a]	Kinetic diameters (Å)[b]
Nap		128	3.29	6.55
Ace		154	3.98	6.92
Ant		178	4.54	9.28
Pyr		202	4.88	8.16
FluA		202	5.20	8.78
BaA		228	5.91	10.52

[a] K_{ow}: octanol–water partitioning coefficients from ref. 57 and a databank at http://logkow.cisti.nrc.ca/logkow/search.html. [b] Kinetic diameters from ref. 58 for Nap, Ant, and Pyr, others approximated using simulated with ChemBioOffice 2008 (Cambridge Soft Corporation).

effective to avoid corrosion and oxidation. Fig. 3C shows the size and shape of MIL-101 crystals. $Fe_3O_4@SiO_2$ MMPs were found to be assembled onto the external surface of MIL-101 crystals under ultrasonication of a mixture of $Fe_3O_4@SiO_2$ and MIL-101 dispersion in aqueous solution (Fig. 3D). Thus, the magnetization of MIL-101 was achieved *via* the formation of $Fe_3O_4@SiO_2$–MIL-101 hybrids due to the static electric interaction between the positively charged MIL-101 and negatively charged $Fe_3O_4@SiO_2$ (Fig. 2D).

Effect of the amount of MIL-101

The effect of the amount of MIL-101 on the performance of the $Fe_3O_4@SiO_2$–MIL-101 for MSPE of PAHs was investigated with 20 mL of ultrapure water spiked with PAHs (50 ng mL^{-1} each). PAHs were hardly extracted by $Fe_3O_4@SiO_2$ without adding MIL-101, indicating that MIL-101 played a key role in the adsorption of PAHs on $Fe_3O_4@SiO_2$–MIL-101 (Fig. 4A). The extraction efficiency increased rapidly when the amount of MIL-101 increased from 0 to 0.6 mg, indicating the remarkable enrichment ability of MIL-101. The extraction efficiency increased slightly or even decreased when the MIL-101 amount increased from 0.6 to 1.0 mg, indicating that excessive MIL-101 without magnetic modification adsorbed a part of PAHs which could not be collected by magnetic separation. In the following experiment, 0.6 mg of MIL-101 was employed.

Effect of solution pH

The effect of solution pH on the extraction of PAHs was investigated in a pH range of 3 to 9 (Fig. 4B). PAHs exist as neutral molecules in aqueous solution, which made their adsorption unaffected due to the charge change on the surface of the sorbents. However, solution pH could affect the charges on the surface of SiO_2 and SiO_2/MIL-101, thereby changing the stability of $Fe_3O_4@SiO_2$–MIL-101 formed *via* static electric interaction

Table 2 Figures of merit for the SPME with $Fe_3O_4@SiO_2$–MIL-101 as sorbent for HPLC-PDA determination of PAHs

| PAHs | Linear range ($\mu g\ L^{-1}$) | Precision (RSD, $n = 5$, $1\ \mu g\ L^{-1}$) (%) | | LODs ($ng\ L^{-1}$) | LOQs ($ng\ L^{-1}$) | EFs (mean $\pm$ s, $n = 3$) |
		Intra-day	Inter-day			
Nap	0.01–250	4.3	7.9	2.8	6.3	180 ± 12
Ace	0.1–250	3.1	6.1	15.0	44.2	151 ± 5
Ant	0.01–250	6.4	6.4	5.5	9.3	101 ± 17
FluA	0.01–250	4.8	8.5	3.9	7.8	113 ± 10
Pyr	0.1–250	8.7	8.3	27.2	87.7	108 ± 9
BaA	0.05–250	7.1	6.9	9.8	33.5	150 ± 7

and in turn the MSPE of PAHs. As illustrated in Fig. 4B, there was no significant influence of solution pH from 3 to 6 on the extraction of PAHs. A further increase of pH to 9 led to a slight decrease of the MSPE efficiency of PAHs. The above results can be attributed to the fact that the MIL-101 surface was positively charged when the pH value was below the point of zero charge (9.6) (Fig. 2D), and was more stable from pH 3 to 6. Moreover, the zeta potential of MIL-101 became negative and unstable when the pH value exceeded 9.6.

The results show that the interaction between MIL-101 and PAHs molecules made a principal contribution to the extraction. All of the studied PAHs can enter the pores of MIL-101 as their kinetic dynamic diameters (6.55–10.52 Å) (Table 1) are smaller than the pores (29 Å and 34 Å) and the windows (12 Å and 16 Å × 14.5 Å) of MIL-101.[53] Large octanol–water partitioning coefficients of the PAHs enable their hydrophobic interaction with the hydrophobic MIL-101 framework. The PAHs with highly delocalized π electrons allow π–π interaction with the terephthalic acid molecules in the framework of MIL-101, and the π-complexation between the π-electrons of aromatic rings and the Lewis acid sites in the pores of MIL-101.

Effect of extraction time

Extraction time profiles for the six PAHs are shown in Fig. 4C. The peak areas of the analytes increased as extraction time increased from 5 to 20 min, and remained stable with a further increase of extraction time. The extraction was quite fast as 5 min was sufficient to obtain 65–82% of the maximum peak areas for the analytes, and 20 min for the maximum peak areas. Finally,

25 min was chosen as the extraction time to ensure the extraction equilibrium.

Salt effect

To investigate the salt effect on the extraction of the PAHs, NaCl was used to adjust the solution salinity. As shown in Fig. 4D, the peak areas for the PAHs increased as the concentration of NaCl increased from 0 to 60 mM, then leveled off or even decreased with a further increase of the concentration of NaCl. The effect of salt on the adsorption of PAHs can be twofold. On one hand, the addition of NaCl would decrease the solubility of PAHs in the aqueous phase and enhance the hydrophobic interaction between PAHs and the sorbent, which promoted the MSPE. On the other hand, excessive NaCl would weaken the static electric interaction between $Fe_3O_4@SiO_2$ and MIL-101, and reduce the stability of $Fe_3O_4@SiO_2$–MIL-101 for MSPE. Therefore, 60 mM NaCl was chosen as a compromise in the following extractions.

Choice of solvent for desorption

Three solvents including methanol, acetonitrile and acetone were tested for the desorption of PAHs from $Fe_3O_4@SiO_2$–MIL-101. The desorption capabilities of the above three solvents are compared in Fig. 4E. Under the same extraction and elution conditions, acetonitrile provided the best desorption efficiency due to its strongest dissolving ability towards PAHs. Ultrasonic irradiation and multiple elution were found to facilitate the desorption of PAHs from the sorbent. Triplicate desorptions with 0.5 mL of acetonitrile each time under ultrasonic irradiation

Table 3 Comparison of the LODs obtained with SPE using different sorbents for HPLC determination of PAHs

Sorbent	Mode	Amount of sorbent (mg)	Sample volume (mL)	Technique	LODs ($ng\ L^{-1}$)	Ref.
Fe_3O_4/carbon	MSPE	50	1000	HPLC-FLD	0.2–0.6	37
Fe_3O_4/C_{18}-barium alginate	MSPE	100	500	HPLC-FLD	2–5	38
Tetradecanoate-coated Fe_3O_4	MSPE	200	350	HPLC-FLD	0.1–0.25	39
Ionic liquid-coated Fe_3O_4	MSPE	50 (ionic liquid) + 80 (Fe_3O_4)	300	HPLC-FLD	0.33–8.33	51
Copper isonicotinate coordination polymer	Packed cartridge on-line	200	50	HPLC-PDA	2–14	8
Cigarette filter	Packed cartridge on-line	—	42	HPLC-PDA	0.9–58.6	45
Multiwalled carbon nanotubes	Packed cartridge	100	100	HPLC-UV	5–58	48
Sulfur microparticles	Packed cartridge	1500	100	HPLC-UV	7–48	52
$Fe_3O_4@SiO_2$–MIL-101	MSPE	0.6 (MIL-101) + 1.0 ($Fe_3O_4@SiO_2$)	20	HPLC-PDA	2.8–27.2	This work

Table 4 Analytical results (mean $\pm$ s, $n = 3$) for the determination of PAHs in water samples

Analytes	Lake water 1		Lake water 2		Wastewater	
	Concentration (ng L^{-1})	Recovery^a (%)	Concentration (ng L^{-1})	Recovery^a (%)	Concentration (ng L^{-1})	Recovery^a (%)
Nap	nd^b	86.8 $\pm$ 10.8	nd	98.7 $\pm$ 4.3	58.7 $\pm$ 6.4	105 $\pm$ 3.1
Ace	nd	83.6 $\pm$ 5.4	nd	87.4 $\pm$ 7.5	nd	96.4 $\pm$ 2.2
Ant	44.7 $\pm$ 5.3	94.8 $\pm$ 3.0	nd	95.7 $\pm$ 5.2	60.2 $\pm$ 7.0	84.8 $\pm$ 9.3
FluA	nd	96.4 $\pm$ 6.5	nd	91.1 $\pm$ 3.6	77.1 $\pm$ 8.5	102 $\pm$ 4.4
Pyr	nd	81.3 $\pm$ 7.1	nd	94.9 $\pm$ 3.8	nd	88.2 $\pm$ 5.8
BaA	63.1 $\pm$ 6.6	85.4 $\pm$ 5.7	nd	86.7 $\pm$ 6.5	54.7 $\pm$ 1.8	97.2 $\pm$ 5.0

^{a} For spiked 1 µg L^{-1}. ^{b} Not detected.
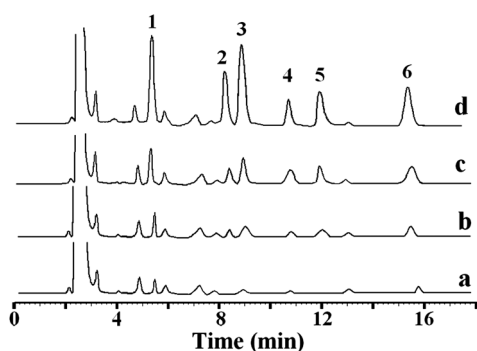
Fig. 5 HPLC chromatograms of the PAHs obtained by the developed method: (a) the wastewater sample; (b) spiked wastewater sample with 0.5 µg L^{-1} of each individual PAHs; (c) spiked wastewater sample with 1.0 µg L^{-1} of each individual PAHs; and (d) spiked wastewater sample with 5.0 µg L^{-1} of each individual PAHs. Peak identity: 1, Nap; 2, Ace; 3, Ant; 4, FluA; 5, Pyr; and 6, BaA.

for 20 s (total 1.5 mL of acetonitrile) enabled quantitative stripping of the adsorbed PAHs from the sorbent (Fig. 4F).

Figures of merit

The figures of merit for the developed MSPE with Fe$_3$O$_4$@SiO$_2$–MIL-101 as the sorbent for HPLC-PDA determination of PAHs are summarized in Table 2. With the consumption of 20 mL sample solution, the enrichment factors of the PAHs, defined as the ratio of the concentration of the analyte in the extract to that in the original sample, ranged from 101 to 180. The intra- and inter-day reproducibility (relative standard deviations, RSDs) was calculated with the PAHs spiked at 1 µg L^{-1} in water. Five parallel extractions of a sample solution over a day gave the intra-day RSDs, and the inter-day RSDs were determined by extracting sample solutions that had been independently prepared for contiguous days. The intra- and inter-day RSDs were in the range of 3.1–8.7% and 6.1–8.5%, respectively, indicating the acceptable reproducibility. The limits of detection (LODs, S/N = 3) and limits of quantification (LOQs, S/N = 10) were found to be 2.8–27.2 ng L^{-1} and 6.3–87.7 ng L^{-1}, respectively. Compared with previous SPE methods using various sorbents for HPLC determination of PAHs, the present method required smaller amounts of the sorbent Fe$_3$O$_4$@SiO$_2$–MIL-101 and smaller sample solution, but generally gave lower LODs with UV and PDA detection (Table 3).

Sample analysis

The developed MSPE with Fe$_3$O$_4$@SiO$_2$–MIL-101 as the sorbent was applied to HPLC determination of PAHs in local water samples. The analytical results are given in Table 4. Four PAHs (Nap, Ant, FluA, and BaA) were detected in the wastewater sample, ranging from 54.7 to 77.1 ng L^{-1}, while the concentrations of Ace and Pyr were below their LODs. Ant and BaA were detected in lake water 1, whereas no PAHs were found in lake water 2. The recoveries for spiked 1 µg L^{-1} PAHs ranged from 81.3% to 105%. Chromatograms of the PAHs in the wastewater sample and their corresponding spiked solutions are shown in Fig. 5.

Conclusions

In this work, we have shown a facile magnetization of MOF MIL-101 for rapid MSPE of PAHs in environmental water samples. The developed approach offers large enrichment factor, wide linear range, and good reproducibility. Owing to the diverse structures and unique characteristics of MOFs, the combination of magnetic separation with MOFs is attractive for rapid and efficient extraction of various trace analytes from environmental and biological samples.

Acknowledgements

References

1 O. M. Yaghi, M. O'Keeffe, N. W. Ockwig, H. K. Chae, M. Eddaoudi and J. Kim, *Nature*, 2003, **423**, 705.
2 M. Eddaoudi, J. Kim, N. Rosi, D. Vodak, J. Wachter, M. O'Keeffe and O. M. Yaghi, *Science*, 2002, **295**, 469.
3 Y. K. Hwang, D.-Y. Hong, J.-S. Chang, S. H. Jhung, Y.-K. Seo, J. Kim, A. Vimont, M. Daturi, C. Serre and G. Férey, *Angew. Chem., Int. Ed.*, 2008, **47**, 4144.
4 B. L. Chen, S. C. Xiang and G. D. Qian, *Acc. Chem. Res.*, 2010, **43**, 1115.
5 Z.-Y. Gu, C.-X. Yang, N. Chang and X.-P. Yan, *Acc. Chem. Res.*, 2012, **45**, 734.
6 Z. Ni, J. P. Jerrell, K. R. Cadwallader and R. I. Masel, *Anal. Chem.*, 2007, **79**, 1290.
7 Z.-Y. Gu, G. Wang and X.-P. Yan, *Anal. Chem.*, 2010, **82**, 1365.
8 Y.-Y. Zhou, X.-P. Yan, K.-N. Kim, S.-W. Wang and M.-G. Liu, *J. Chromatogr., A*, 2006, **1116**, 172.

9 Z.-Y. Gu, Y.-J. Chen, J.-Q. Jiang and X.-P. Yan, *Chem. Commun.*, 2011, **47**, 4787.

10 X.-Y. Cui, Z.-Y. Gu, D.-Q. Jiang, Y. Li, H.-F. Wang and X.-P. Yan, *Anal. Chem.*, 2009, **81**, 9771.

11 N. Chang, Z.-Y. Gu, H.-F. Wang and X.-P. Yan, *Anal. Chem.*, 2011, **83**, 7094.

12 D. Ge and H. K. Lee, *J. Chromatogr., A*, 2011, **1218**, 8490.

13 B. Chen, C. Liang, J. Yang, D. S. Contreras, Y. L. Clancy, E. B. Lobkovsky, O. M. Yaghi and S. Dai, *Angew. Chem., Int. Ed.*, 2006, **45**, 1390.

14 J.-R. Li, J. Sculley and H.-C. Zhou, *Chem. Rev.*, 2012, **112**, 869.

15 Z.-Y. Gu, D.-Q. Jiang, H.-F. Wang, X.-Y. Cui and X.-P. Yan, *J. Phys. Chem. C*, 2010, **114**, 311.

16 N. Chang, Z.-Y. Gu and X.-P. Yan, *J. Am. Chem. Soc.*, 2010, **132**, 13645.

17 Z.-Y. Gu, J.-Q. Jiang and X.-P. Yan, *Anal. Chem.*, 2011, **83**, 5093.

18 L. Alaerts, C. E. A. Kirschhock, M. Maes, M. A. van der Veen, V. Finsy, A. Depla, J. A. Martens, G. V. Baron, P. A. Jacobs, J. F. M. Denayer and D. E. De Vos, *Angew. Chem., Int. Ed.*, 2007, **46**, 4293.

19 C.-X. Yang and X.-P. Yan, *Anal. Chem.*, 2011, **83**, 7144.

20 C.-X. Yang, Y.-J. Chen, H.-F. Wang and X.-P. Yan, *Chem.–Eur. J.*, 2011, **17**, 11734.

21 C.-X. Yang, S.-S. Liu, H.-F. Wang, S.-W. Wang and X.-P. Yan, *Analyst*, 2012, **137**, 133.

22 S.-S. Liu, C.-X. Yang, S.-W. Wang and X.-P. Yan, *Analyst*, 2012, **137**, 816.

23 M. R. Lohe, K. Gedrich, T. Freudenberg, E. Kockrick, T. Dellmann and S. Kaskel, *Chem. Commun.*, 2011, **47**, 3075.

24 F. Ke, Y.-P. Yuan, L.-G. Qiu, Y.-H. Shen, A.-J. Xie, J.-F. Zhu, X.-Y. Tian and L.-D. Zhang, *J. Mater. Chem.*, 2011, **21**, 3843.

25 K. Aguilar-Arteaga, J. A. Rodriguez and E. Barrado, *Anal. Chim. Acta*, 2010, **674**, 157.

26 X.-L. Zhang, H.-Y. Niu, W.-H. Li, Y.-L. Shi and Y.-Q. Cai, *Chem. Commun.*, 2011, **47**, 4454.

27 J.-H. Lin, Z.-H. Wu and W.-L. Tseng, *Anal. Methods*, 2010, **2**, 1874.

28 Y.-B. Luo, Z.-G. Shi, Q. Gao and Y.-Q. Feng, *J. Chromatogr., A*, 2011, **1218**, 1353.

29 H.-F. Zhang and Y.-P. Shi, *Analyst*, 2012, **137**, 910.

30 X.-S. Li, J.-H. Wu, L.-D. Xu, Q. Zhao, Y.-B. Luo, B.-F. Yuan and Y.-Q. Feng, *Chem. Commun.*, 2011, **47**, 9816.

31 Q. Liu, J. B. Shi, M. T. Cheng, G. L. Li, D. Cao and G. B. Jiang, *Chem. Commun.*, 2012, **48**, 1874.

32 F. Bianchi, V. Chiesi, F. Casoli, P. Luches, L. Nasi, M. Careri and A. Mangia, *J. Chromatogr., A*, 2012, **1231**, 8.

33 J. Ding, Q. Gao, D. Luo, Z.-G. Shi and Y.-Q. Feng, *J. Chromatogr., A*, 2010, **1217**, 7351.

34 Q. Gao, C.-Y. Lin, D. Luo, L.-L. Suo, J.-L. Chen and Y.-Q. Feng, *J. Sep. Sci.*, 2011, **34**, 3083.

35 F. Yang, Y. M. Long, R. Shen, C. Y. Chen, D. Pan, Q. L. Zhang, Q. Y. Cai and S. Z. Yao, *J. Sep. Sci.*, 2011, **34**, 716.

36 Y. Liu, H. Li and J.-M. Lin, *Talanta*, 2009, **77**, 1037.

37 S. Zhang, H. Niu, Z. Hu, Y. Cai and Y. Shi, *J. Chromatogr., A*, 2010, **1217**, 4757.

38 S. Zhang, H. Niu, Y. Cai and Y. Shi, *Anal. Chim. Acta*, 2010, **665**, 167.

39 A. Ballesteros-Gómez and S. Rubio, *Anal. Chem.*, 2009, **81**, 9012.

40 M. Chorąży, J. Szeliga, M. Stróżyk and B. Cimander, *Environ. Health Perspect.*, 1994, **102**, 61.

41 L. Wolska, K. Galer, T. Górecki and J. Namieśnik, *Talanta*, 1999, **50**, 985.

42 Q. Zhao, F. Wei, Y.-B. Luo, J. Ding, N. Xiao and Y.-Q. Feng, *J. Agric. Food Chem.*, 2003, **59**, 12794.

43 H. Zhang, W.-P. Low and H.-K. Lee, *J. Chromatogr., A*, 2012, **1233**, 16.

44 C.-H. Xiao, S.-Q. Han, Z.-Y. Wang, J. Xing and C.-Y. Wu, *J. Chromatogr., A*, 2001, **927**, 121.

45 H.-D. Liang, D.-M. Han and X.-P. Yan, *J. Chromatogr., A*, 2006, **1103**, 9.

46 Z. L. Chen, M. Megharaj and R. Naidu, *Chromatographia*, 2002, **56**, 105.

47 S. S. Segro, Y. Cabezas and A. Malik, *J. Chromatogr., A*, 2009, **1216**, 4329.

48 W.-D. Wang, Y.-M. Huang, W.-Q. Shu and J. Cao, *J. Chromatogr., A*, 2007, **1173**, 27.

49 H.-L. Xu, Y. Li, D.-Q. Jiang and X.-P. Yan, *Anal. Chem.*, 2009, **81**, 4971.

50 F. Gosetti, U. Chiuminatto, E. Mazzucco, E. Robotti, G. Calabrese, M. C. Gennaro and E. Marengo, *J. Chromatogr., A*, 2011, **1218**, 6308.

51 Q. Zhang, F. Yang, F. Tang, K. Zeng, K. Wu, Q. Cai and S. Yao, *Analyst*, 2010, **135**, 2426.

52 V. Khalili-Fard, K. Ghanemi and Y. Nikpour, *Anal. Chim. Acta*, 2012, **714**, 89.

53 O. I. Lebedev, F. Millange, C. Serre, G. Van Tendeloo and G. Férey, *Chem. Mater.*, 2005, **17**, 6525.

54 H. Deng, X. L. Li, Q. Peng, X. Wang, J. P. Chen and Y. D. Li, *Angew. Chem., Int. Ed.*, 2005, **44**, 2782.

55 W. Stöber and A. Fink, *J. Colloid Interface Sci.*, 1968, **26**, 62.

56 Y. H. Deng, C. C. Wang, J. H. Hu, W. L. Yang and S. K. Fu, *Colloids Surf., A*, 2005, **262**, 87.

57 A. A. Meharg, J. Wright, H. Dyke and D. Osborn, *Environ. Pollut.*, 1998, **99**, 29.

58 R. Ahmad, A. G. Wong-Foy and A. J. Matzger, *Langmuir*, 2009, **25**, 11977.